SUPPLEMENTAL METHODS:

Reagents: IL-17A, IL-17F, IL-22, IL-23, TGF-β1, IL-6, Leptin were purchased from R&D. Anti-IL-6 Ab was purchased from eBioscience. PMA, Ionomycin are gift of Dt. Karin.

Detection of IL-17RA mRNA in patients with alcohol-induced liver fibrosis. Liver biopsy specimens were obtained during routine diagnostic and immediately frozen in liquid nitrogen. Alcoholic liver lesions were assessed according to Kleiner et al[1], and fibrosis stages were defined as F0 (n=2), F1 (n=5), F2 (n=5), F3 (n=4). For quantification of mRNA expression, total RNA was isolated from snap frozen tissues mRNA was using the RNeasy kit (Qiagen, Basel, Switzerland) and converted to cDNA. Quantitative real-time PCR was performed on the ABI 7700 Sequence Detector (Applied Biosystems, Rotkreuz, Switzerland) with ready-to-use primers and probe kits for human IL-17RA (Applied Biosystems, Rotkreuz, Switzerland), and normalized to GAPDH. The human study was approved by the local Ethics Committee of the University of Heidelberg, Germany, where all biopsies were carried out; all patients gave written informed consent to have their tissues included in the study.

Primary Cell cultures: Primary HSCs and KC were isolated from the wild type and were used for flow cytometry analysis or cultured on uncoated plastic tissue culture dishes in Dulbecco's modified Eagle's medium (DMEM; Gibco-BRL, Grand Island, NY) supplemented with 10% fetal calf serum (FCS), 2 mM L-glutamine and standard antibiotics. Hepatocytes were cultured on collagen-coated plastic plates in Waymouth's medium supplemented with 10% FCS.

RT-PCR and real time quantitative PCR. mRNA was isolated and RT-PCR was performed using ABI 7000 sequence detection system (Applied Biosystems), specific primers and SYBRGreen. Ct values of each sample were normalized to 18s mRNA

expression. Values were expressed as fold induction in comparison with untreated or sham controls. Primers used for RT-PCR:.

Gene	RefSeq ID:	Forward	Reverse
m IL-17Ra	NM_008359	CTTGACTCTGCAGCTCAGCC	ATGGCTGCTTCTGCTGCT
m IL-17Rc	NM_134159	CCTGCTCCTCAGAGACATCC	ATCTGGTCCTACACGAAGCC
m IL-17A	NM_010552	TGAGCTTCCCAGATCACAGA	TCCAGAAGGCCCTCAGACTA
m IL-17F	NM_145856	TTGATGCAGCCTGAGTGTCT	AATTCCAGAACCGCTCCAGT
m IL-6	NM_031168	ACCAGAGGAAATTTTCAATAGGC	TGATGCACTTGCAGAAAACA
m IL-1-β	NM_008361	GGTCAAAGGTTTGGAAGCAG	TGTGAAATGCCACCTTTTGA
m TGF-β1	NM_011577	CAACCCAGGTCCTTCCTAAA	GGAGAGCCCTGGATACCAAC
m TNF-α	NM_013693	AGGGTCTGGGCCATAGAACT	CCACCACGCTCTTCTGTCTAC
m MMP3	NM_010809	AGCCTTGGCTGAGTGGTAGA	CGATGATGAACGATGGACAG
m COLIA1	NM_007742	TAGGCCATTGTGTATGCAGC	ACATGTTCAGCTTTGTGGACC
m TIMP1	NM_001044384	AGGTGGTCTCGTTGATTCGT	GTAAGGCCTGTAGCTGTGCC
m α-SMA	NM_007392	GTTCAGTGGTGCCTCTGTCA	ACTGGGACGACATGGAAAAG
m18S rRNA	NM_025447	AGTCCCTGCCCTTTGTACACA	CGATCCGAGGGCCTCACTA
h IL-6	NM_000600	GTCAGGGGTGGTTATTGCAT	AGTGAGGAACAAGCCAGAGC
h IL-8	NM_000584.2	AAATTTGGGGTGGAAAGGTT	TCCTGATTTCTGCAGCTCTGT
h TGF-β1	NM_000660.3	GCCCTGGACACCAACTATTGCT	AGGCTCCAAATGTAGGGGCAGG
h COL1A1	NM_000088.3	CACACGTCTCGGTCATGGTA	AAGAGGAAGGCCAAGTCGAG
mIL-22	----------	ACAGGTTCCAGCCCTACATG	GTCGTCACCGCTGATGTG
mIL-25	----------	CCAGGTGGTTGCATTCTTGG	TGGCTGTAGGTGTGGGTTCC
mIL-23a	----------	GAACGCACATGCACCAGCGG	TGCAAGCAGAACTGGCTGTTGTCC
h TIMP1	NM_003254.2	AGGTGGTCTCGTTGATTCGT	GTAAGGCCTGTAGCTGTGCC
h SMA	NM_001141945.1	CCAGAGCCATTGTCACACAC	CAGCCAAGCACTGTCAGG
h IL-17A	NM_002190.2	CACTTTGCCTCCCAGATCAC	ACCAATCCCAAAAGGTCCTC
h IL-17F	NM_052872.3	CCTCACTCAGAAAGGCAAGC	AGCGCAACATGACAGTGAAG

Whole Mouse Genome Gene Expression Microarray: The gene expression profile of HSCs was studied using Whole Mouse Genome Microarray (Agilent). For this purpose, Vitamin A^+YFP^+ and Vitamin A^+YFP^- HSCs were sort purified from Collagen-α2(I)$^{Cre\text{-}YFP}$ mice with no injury, after CCl_4 (2 mo), and after 7 days or 1 mo recovery from CCl_4. mRNA was purified using RNAeasy columns (Qiagen, Valencia, CA), 160 ng of purified RNA per sample was labeled using the LRILAK PLUS, two color low RNA input Linear Amplification kit and hybridized to a Whole Mouse Genome Microarray 4x44K 60 mer slide according to the manufacturer's instructions (Agilent, Santa Clara, CA). Slides were scanned using the Agilent GZ505B Scanner and analyzed using the Gene Spring Software (Agilent). Hierarchical clustering of gene expression values was performed using Cluster 3.0 (http://bonsai.hgc.jp/~mdehoon/software/cluster/software.htm,[2]) using the correlation coefficient as the similarity metric, and average linkage when merging

nodes during tree building. Clustering was performed on genes expressed in at least one condition (>9 $\log_2$ intensity value) to remove absent genes and genes exhibiting a standard deviation greater than 0.75 among $\log_2$ intensity values to remove genes with constant expression. Hierarchical clustering results were visualized using Java Tree View (http://jtreeview.sourceforge.net/, [3]). Differentially regulated genes were defined as those with significant absolute expression (>9 $\log_2$ intensity value) and exhibiting 2-fold compared to the maximal value in all other samples. Gene ontology and KEGG pathway functional enrichment analysis was performed using DAVID (http://david.abcc.ncifcrf.gov, [4]).

Western blot analysis was performed using protein lysates from IL-17A-stimulated primary cells or cell lines. Phospho-ERK, total ERK, phospho-AKT (on Ser473), AKT1, phospho-JNK, total-JNK, phospho-NF-κB (p65), NF-κB (p65), phospho-Stat3, Stat3 (Cell Signaling Technologies, Inc.) and α-Tubulin (Santa Cruz) were used and visualized them by the enhanced chemiluminescence light method (Amersham Biosciences).

Flow cytometry: Lymphoid fraction from untreated (n=3) and BDL-injured (n=3) wild type mice were *in vitro* stimulated with PMA (100ng/ml) + Ionomycin (500ng/ml) + Brefeldin A (or IL-23 + Brefeldin A) for 5h, and analyzed by flow cytometry for intracellular IL-17A and IL-17F expression. Phenotyping of the lymphoid cell fraction isolated from mouse liver was performed on BD LSR II (BD Bioscience Flow Cytometry Systems, BD) using anti-mouse CD90.2-PE, CD4–PE, CD3-PE, CD8α-FITC, CD8a-APC, CD4-PerCp-Cy5.5, CD11b-eFluor™ 450, CD11b-FITC, B200-APC, CD11b-PE-Cy5, NK1.1-PE-Cy7, CD45R(B220)-PE-Cy7, F4/80-PerCP-Cy5.5, F4/80-PE, CD11c-PE-Cy7, CD11c-APC, CD11c-PE, CD8a-FITC, IL-17A-Alexa647, IL-17F-PE Abs

(eBioscience, San Diego, CA). Intracellular staining was performed using BD Cytofix/Cytoperm fixation and Permeabilization Solution (BD, San Jose, CA).

ACKNOWLEDGMENTS

We thank Dr. Yanagida (Kyoto University), and Karin Diggle (UCSD) for support. This study was supported by the National Institutes of Health (GM41804, AA15055, DK72237, AI077780), the American Liver Foundation (2006 Liver Scholar Research Award), Shandong Province Science and Technology Plan (2006GG2202042) and Key Project of Chinese Ministry of Science and Technology (2008ZX10002-007), IK99DK088589-01A1, CCFA#2693.

REFERENCES:

1. Kleiner DE, Brunt EM, Van Natta M, et al. Design and validation of a histological scoring system for nonalcoholic fatty liver disease. Hepatology 2005;41:1313-21.
2. de Hoon MJ, Imoto S, Nolan J, et al. Open source clustering software. Bioinformatics 2004;20:1453-4.
3. Saldanha AJ. Java Treeview--extensible visualization of microarray data. Bioinformatics 2004;20:3246-8.
4. Dennis G, Jr., Sherman BT, Hosack DA, et al. DAVID: Database for Annotation, Visualization, and Integrated Discovery. Genome Biol 2003;4:P3.

SUPPLEMENTAL FIGURE LEGEND:

Supplemental Figure 1. Upregulation of IL-17A levels in patients liver fibrosis and cirrhosis.

(A) Human liver tissues were obtained from patients with hepatitis C, diagnosed with clinical and pathological stages of liver fibrosis (F1) and cirrhosis (F4), or no fibrosis (F0), and analyzed by immunihistochemistry for expression of human IL-17A and Sirius Red staining. Representative images are shown using x 4, 10 and 20 objectives.

(B) Liver biopsy specimens were obtained from alcoholic patients diagnosed with F0 (n=2); F1 (n=5); F2 (n=5); F3 (n=4) stages of liver cirrhosis. mRNA was isolated from frozen liver biopsy tissues and analyzed by RT-PCR for IL-17RA expression.

Supplemental Figure 2. Intracellular IL-17A expression was detected in BDL-injured wild type but not IL-17A-/- mice. Lymphoid fraction from BDL-injured (n=3) wild type mice were *in vitro* stimulated with PMA (100ng/ml) + Ionomycin (500ng/ml) for 5h, and analyzed by flow cytometry for intracellular IL-17A expression. IL-17A expression was detected in hematopoietic cells stained positive for lineage markers (B220, F4/80, CD3ε, CD11b, TCRb), and T cell marker CD90.2. Representative dot plots are shown.

Supplemental Fugure 3. IL-17A induces IL-17A and IL-1β1 production in peritoneal macrophages. Peritoneal macrophages were isolated from thioglycollate-treated mice (6 days), cultured for 48h in DMEM +10% FCS, then transferred to 1%FSC

for 1h and stimulated with IL-17A (10ng/ml) for 6h. Cell lysates were analyzed by ELISA (eBioscience), *p<0.05.

Supplemental Figure 4. Endothelial Cells (EC) express IL-17RA but do not respond to IL-17A stimulation. Primary wild type EC were *in vitro* stimulated with IL-17A (10ng/ml), IL-17F (10 ng/ml), or combination of both. mRNA levels of IL-17A and IL-17RA are shown as fold induction compared with untreated cells, p value is non significant (ns).

Supplemental Figure 5. IL-17 signaling is abrogated in IL-17RA$^{-/-}$ HSCs and Kupffer cells. Primary HSCs and Kupffer cells were isolated from wild type of IL-17RA$^{-/-}$ mice and stimulated with IL-17A. The lack of response in IL-17RA$^{-/-}$ cells indicates that 1) IL-17A regulates IL-17RA expression, 2) that deletion of IL-17RA$^{-/-}$ in these cells makes them insusceptible to IL-17A signaling. The data are shown as fold mRNA induction compared with untreated HSCs, *p<0.02.

Supplemental Figure 6. Generation of BM chimeric mice.

(A) Recipient mice were intravenously injected with liposomal clodronate (150 µl) to deplete Kupffer cells. BMT was performed 24 h later by transplantation of the whole BM into lethally irradiated (1200 Rad) recipient mice.

(B) The efficiency of reconstitution BM was analyzed by flow cytometry in the wild type recipient mice transplanted with the β-actin-RFP BM. 90 ± 2% of RFP^{+} cells were detected in the peripheral blood on chimeric β-actin-RFP→wt mice

(vs 92 ± 3% of RFP^+ cells in β-actin-RFP mice), indicating that 97.8% of BM reconstitution was achieved. Representative dot plots are shown.

(C) The efficiency of Kupffer cell reconstitution was analyzed by immunostaining for F4/80 of the clodronate-pretreated lethally irradiated wild type recipient mice transplanted with the β-actin-RFP BM. 92 ± 4% of Kupffer cell reconstitution was achieved. Representative images are shown using x 40 objective.

Supplemental Figure 7. IL-17A activates Stat3 and NF-κB in KC and HSCs.

(A) Primary murine KC and HSCs were isolated from BDL and CCl_4-treated IL-$17RA^{-/-}$→wt mice. Their activation was accessed by expression of inflammatory genes by quantitative RT-PCR, *p<0.01.

(B) IL-17A induces TGF-β1 production in KC and peritoneal macrophages. Primary KC (from untreated wild type mice) and peritoneal macrophages (from thioglycollate-treated mice) were cultured for 48h in DMEM +10% FCS, then transferred to 1% FSC for 1h and stimulated with IL-17A (10 ng/ml) for an additional 6h. Supernatants (triplicates) were analyzed by ELISA for activated TGF-β1, *p<0.05, **p<0.01.

(C) IL-17A produced by KC (KC) stimulates wild type but not IL-$17RA^{-/-}$ HSCs. Wild type or IL-17RA-deficient KC were stimulated with IL-17A for 6 h, washed and co-cultured with the Col-GFP or Col-$GFP^{IL\text{-}17RA\text{-}/\text{-}}$ HSCs. The number of activated HSCs was estimated by fluorescent microscopy 24 hr after co-culture, and shown as a percent of collagen-α1(I)-GFP^+ cells using x 20 objective.

Representative images are shown, $p<0.05$ compared with co-culture of wt:wt cells.

(D) Primary murine HSCs were isolated from BDL and CCl_4-treated Wt→IL-17RA$^{-/-}$ mice. Their activation was accessed by expression of fibrogenic genes by quantitative RT-PCR, *$p<0.01$; #$p<0.05$.

(E) Phosphorylation of Stat3, ERK, JNK, AKT was analyzed in IL-17A- (10 ng/ml) stimulated KC (5 x 10^5 cells) and HSCs (5 x 10^5 cells). The protein level was controlled for each sample by α-tubulin expression.

(F) KC activate multiple signaling pathways in response to IL-17A stimulation. Primary KC were isolated from non-injured wild type mice, cultured for 24h, then stimulated with IL-17A (10 ng/ml) and IL-17F (10 ng/ml) ± inhibitors. U0126 (MEK1/2 inhibitor; (2uM), EMD), AZD1480 (Jak1/2 inhibitor; (0.5uM) XX), SB (p38 inhibitor, (2uM), EMD). Cells were pre-incubated with inhibitors for 20 minutes prior to stimulation with IL-17A + IL-17F for 2 h. Expression of fibrogenic and pro-inflammatory cytokines was detected in KC by RT-PCR. *$p<0.05$ and ns – $p>0.05$, calculated in comparison with KC stimulated with IL17A+F.

Supplemental Figure 8. IL-17 signaling activates HSCs.

(A) Schematic representation of the effects of IL-17A signaling on liver fibrogenesis in response to injury. BM-derived cells are the major source of IL-17A. IL-17A regulates production of TGF-β1 by BM-derived macrophages and Kupffer cells, which in turn, stimulate activation of HSC into fibrogenic myofibroblasts via

Smad2/3 signaling pathway and further facilitate differentiation of IL-17A-producing cells. In addition, IL-17A stimulates collagen-α1(I) production in HSCs via Stat3 signaling pathway.

(B) IL-17 signaling induces activation of LX-2 human HSC cell line IL-17A (10 ng/ml, 72h) or IL-17F (10 ng/ml, 72h) induce mRNAs of fibrogenic genes compared with non-stimulated cells, $p<0.05$.

(C) IL-17 signaling induces activation of hTERT human HSC cell line. IL-17A (10 ng/ml, 8h) and IL-17F (10 ng/ml, 8h) induce mRNAs of fibrogenic and inflammatory cytokines compared with non-stimulated cells, detected by RT-PCR, $p<0.03$. Human IL-17A induced nuclear translocation of Stat3 in hTERT cells was observed 30 min after stimulation, representative images are taken using x 20 objective.

SUPPLEMENTAL FIGURES

Supplemental Figure 1

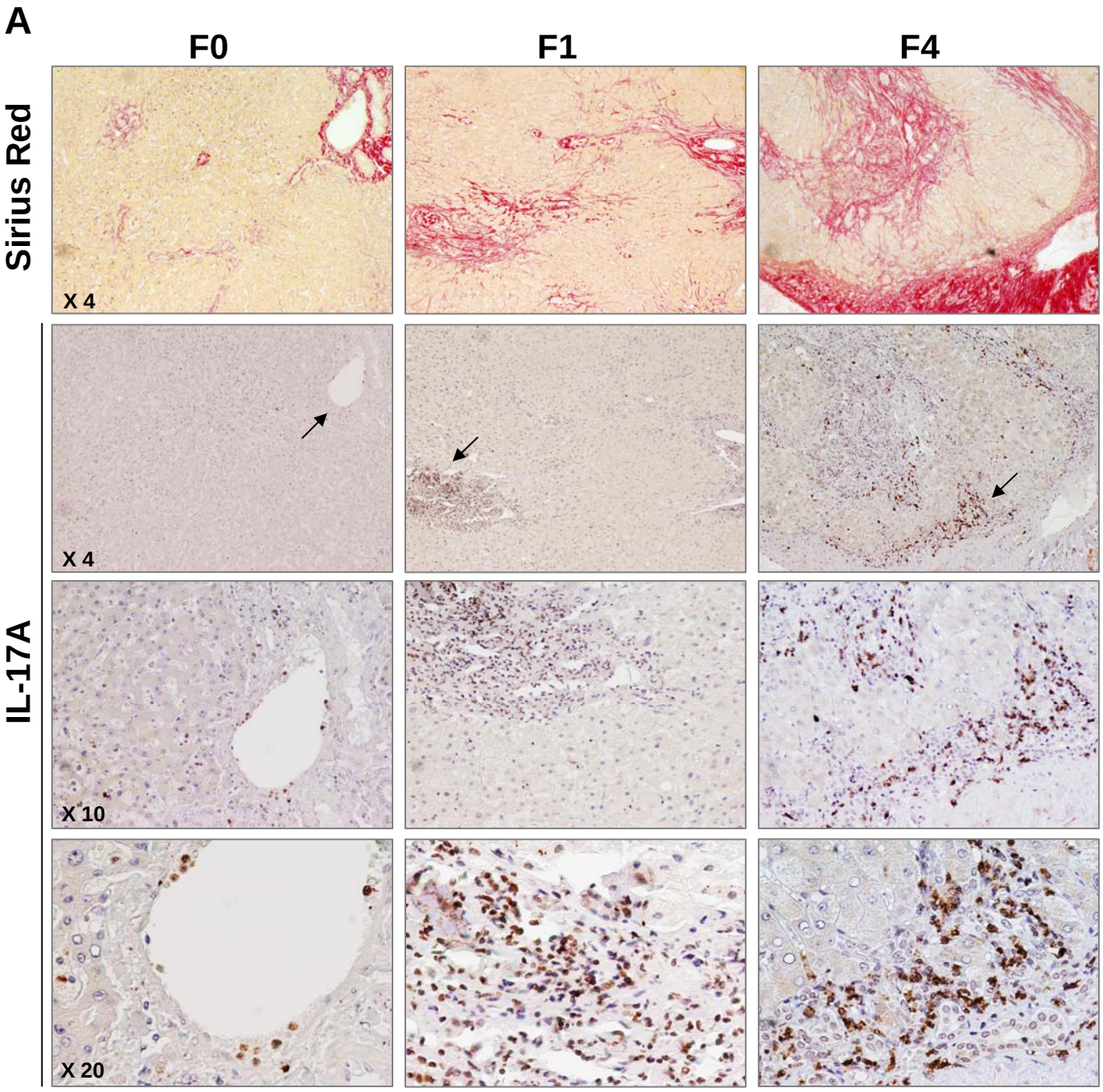

Supplemental Figure 2

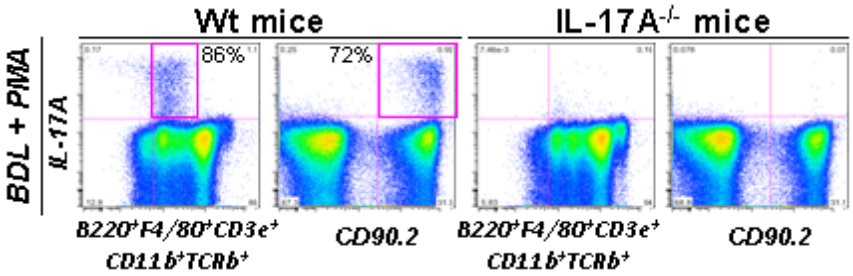

Supplemental Figure 3

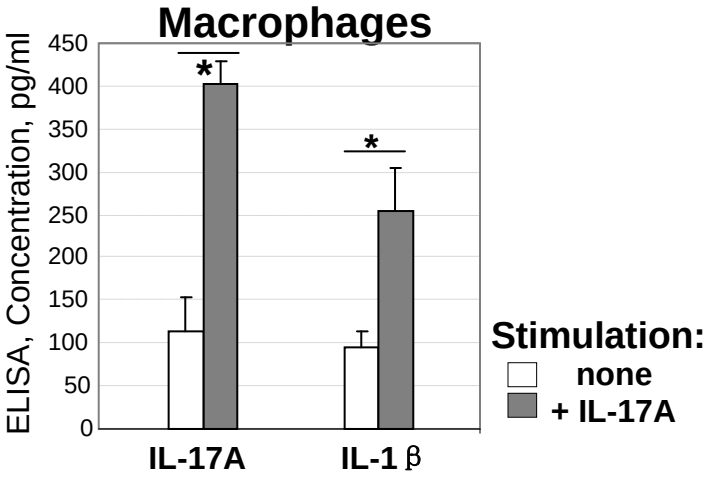

Supplemental Figure 4

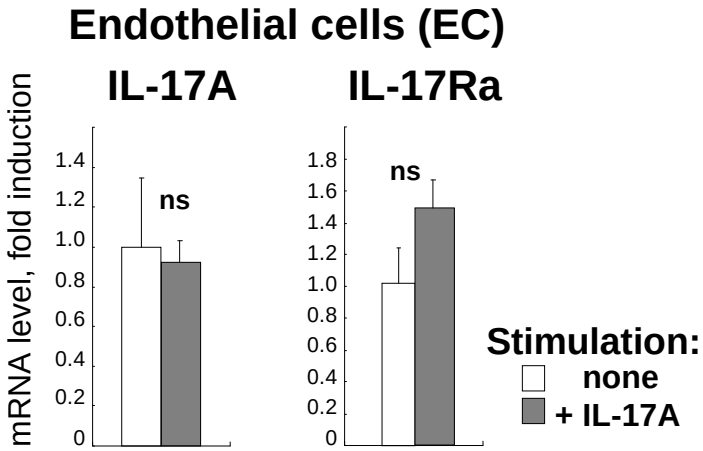

Supplemental Figure 5

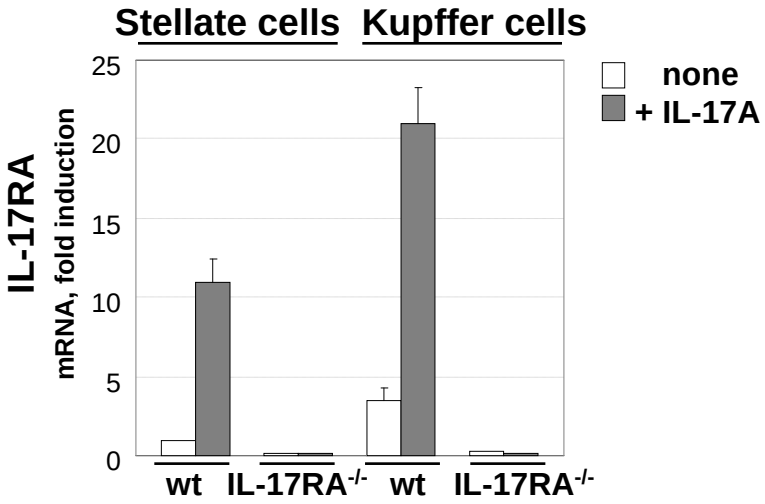

Supplemental Figure 6

A

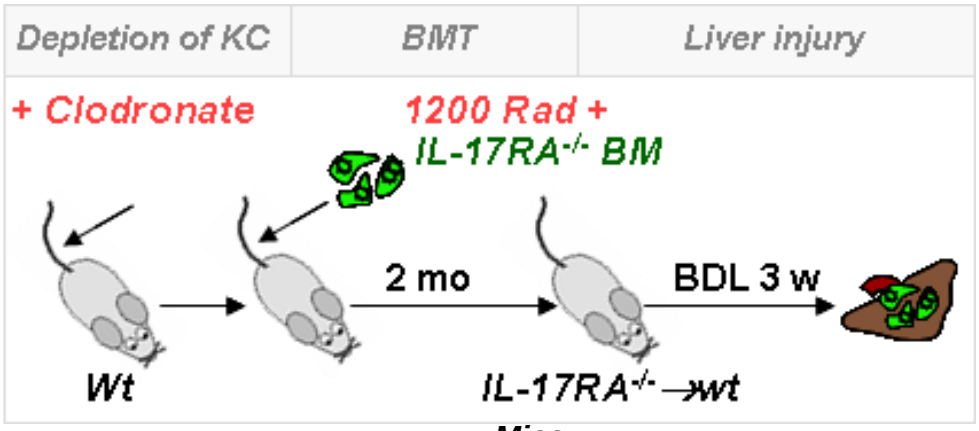

B

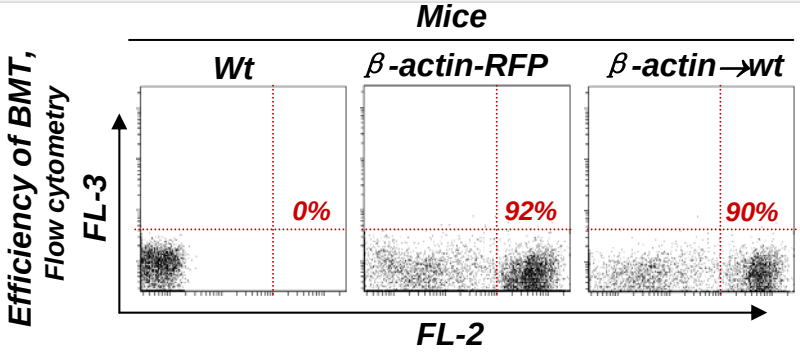

C

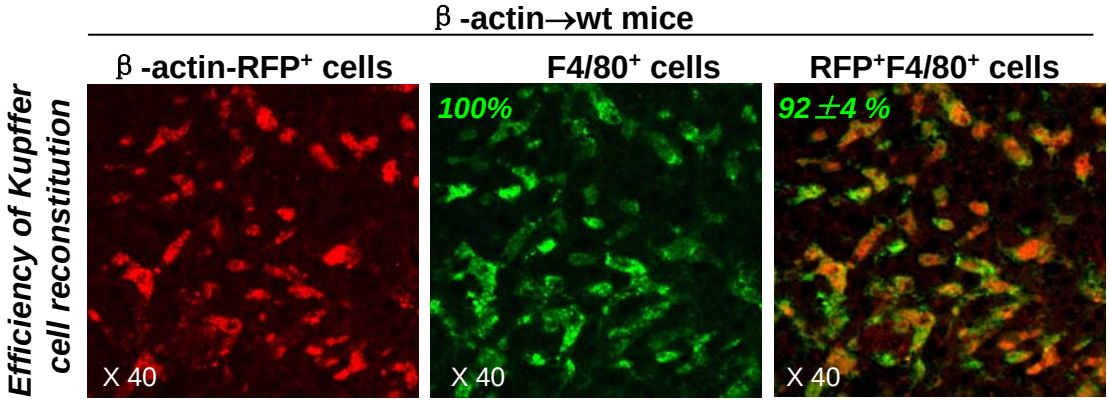

Supplemental Figure 7

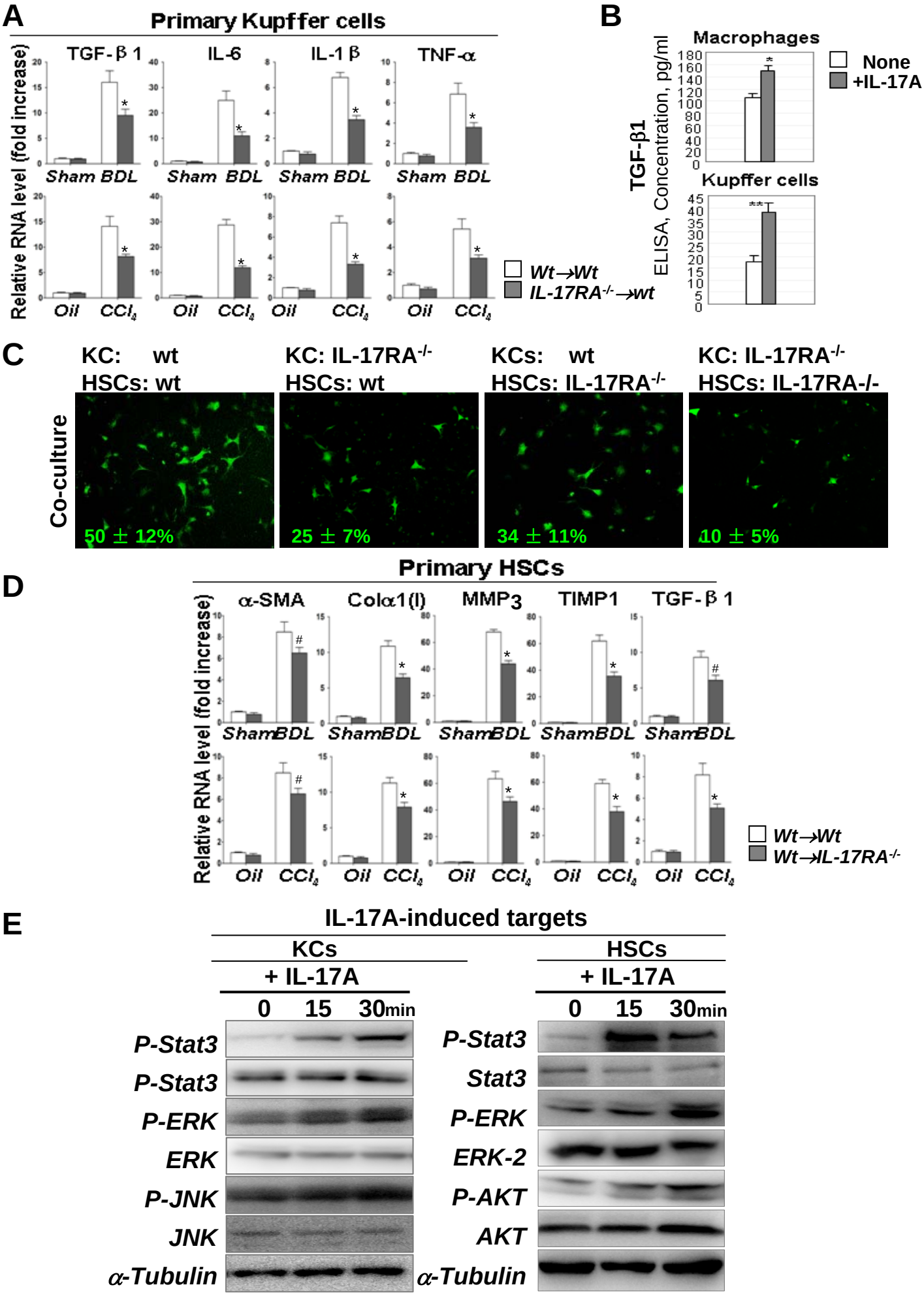

F

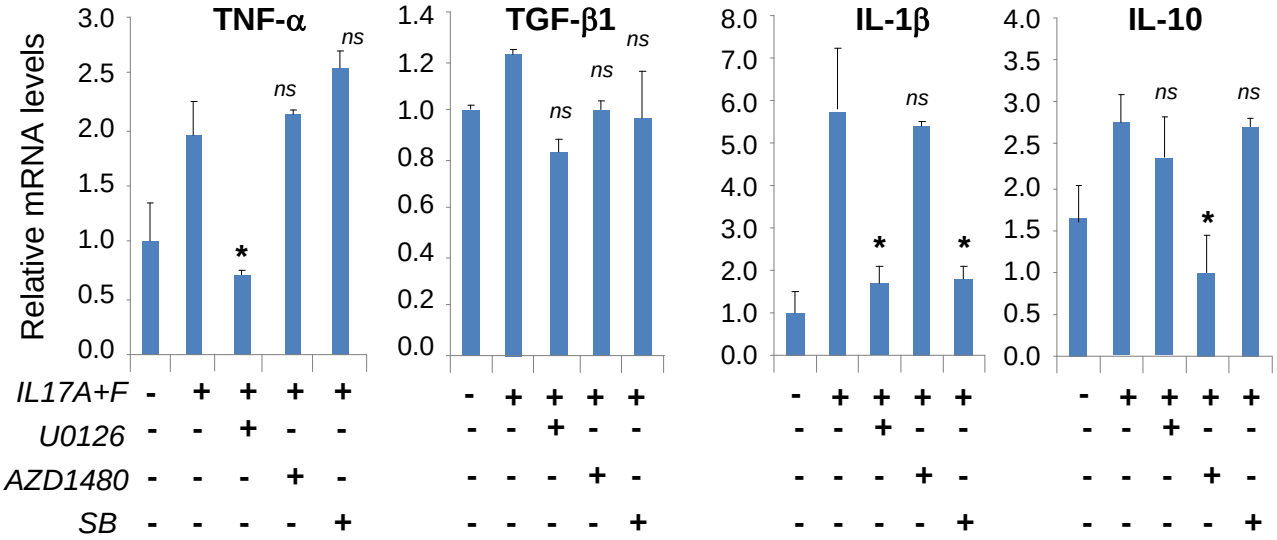
Relative mRNA levels
TNF-α
TGF-β1
IL-1β
IL-10
ns
*
IL17A+F
U0126
AZD1480
SB

Supplemental Figure 8